AUT Journal of Modeling and Simulation

AUT J. Model. Simul., 55(2) (2023) 201-214
DOI: 10.22060/miscj.2024.21827.5304

Process Fault and Homoclinic explosion in the Lorenz system

Zahra Shams, Hassan Zarabadipour*

Department of Electrical Engineering, Faculty of Engineering, Imam-Khomeini International University, Qazvin, Iran.

ABSTRACT: This paper deals with the problem of process faults in the Lorenz system that can affect any of the system parameters and cause the system to exhibit various behaviors. In this paper, the homoclinic orbits in the Lorenz system are described and then the occurrence of process faults in the system is investigated that can cause a homoclinic explosion, bifurcation, change of fixed point, or even instability in the system. In such systems, where a small change in one of the parameters causes large changes in the behavior of the system, to prevent disaster in industrial systems and also to stop the propagation of faults in the system, the faults must be identified as soon as possible. In this paper, the states in the system are estimated by using a reduced-order observer, and the faults are detected. The purpose of this article is to recognize the change in behavior of this system in the face of this type of fault and to express the importance of timely detection and identification of faults in the system so as not to lead to failure and disaster in industrial systems. Finally, the effect of process fault, disturbance, and sensor fault are investigated simultaneously and the states and faults in the system are estimated.

Review History:

Received: Oct. 08, 2022
Revised: Dec. 12, 2023
Accepted: Feb. 04, 2024
Available Online: May, 30, 2024

Keywords:

Process Fault
Estimation
Homoclinic Explosion
Bifurcation
Chaotic Lorenz System

1- Introduction

Faults are any malformed aberration from what is normal or expected. This is one of the most important threats to system reliability because faults can reduce system performance and in industries, they often lead to unfavorable responses that can have catastrophic consequences [1]. Many researchers have studied fault detection approaches and proposed various methods for diagnosing and estimating it [2-5]. Among all these methods, fault estimation (FE) methods have received more attention because they provide more information about the faults that have occurred in the system and have been extensively reviewed over the past 30 years, and many FE procedures have been presented in many fields [6-10].

Among all the diagnostic procedures, observer-based methods achieved increasing research attention recently [11]. In this regard, the fault is detected based on sliding mode observer [12], adaptive observer [13], real-time weighted observer [14], robust L1 observer [15], and optimal state observers [16]. Fault estimation schemes based on an intermediate estimator and an observer are presented in [6] and [8] respectively, to estimate fault signals and the system states simultaneously. A Takagi-Sugeno (TS) fuzzy Proportional-Integral (PI) observer that can detect and estimate the faults and states in the system is investigated in [17]. An interval TS Unknown Input Observer (UIO) is designed in [18] to estimate states and fault signals in an uncertain system. A state estimator is proposed in [19] with intermittent, random actuator faults in networked systems. In [20], a PI observer is used for diagnosing faults in the Lorenz system with bifurcation problems.

Weather with unpredictable behavior, known as a chaotic system, in 1963 Lorenz developed a simple model to describe it [21]. Studying the behavior of physical systems in a number of them such as economic, communication, mechanical, thermal, and electrical systems, chaotic behavior is widely seen [22-25]. Lorenz model [21], which has become a model for chaotic dynamics, explains fluid motion under Rayleigh–Bénard flow conditions [26]. The relationship between temperature deviation and fluid motion, which makes the Lorenz model nonlinear, should be considered to detect the items that caused chaotic dynamics [27]. Chaos can cause risks in system performance and is usually unpredictable because it is sensitive to the initial conditions, therefore research on how to diminish and suppress chaotic behavior is important [28]. Various control methods and procedures have been proposed for the control and regulation of chaotic systems, such as switching control [29], fuzzy control [30], and sliding mode control [31].

Dividing a structure into two portions is the most straightforward definition of the bifurcation term. A slight change in one of the parameters of the dynamical system can have a significant impact on the outcome [32]. Lorenz

*Corresponding author's email: hzarabadi@eng.ikiu.ac.ir

demonstrated that small changes in initial conditions can lead to significant behavioral changes in the system over time [21]. The variation in direction caused by a slight variation in the parameter space can explain the concept of a homoclinic orbit. These orbits are challenging to calculate numerically due to their sensitivity to round-off errors and the limited machine accuracy. However, they become numerically visible with small perturbations, making the occurrence of a homoclinic bifurcation likely [33]. The authors of this article have provided a detailed analysis of the homoclinic bifurcation of the Lorenz system [34].

This article is motivated by two main factors. Firstly, the existing literature on the Lorenz system lacks in-depth exploration and discussion of the effects of faults on the system. The range of behavioral changes resulting from faults has not been thoroughly investigated. This research gap prompted the need for further analysis and investigation. Secondly, previous articles have not adequately emphasized the importance of fault detection in relation to the various effects of different faults. Understanding the specific consequences of different faults is crucial for effective fault detection and mitigation strategies. Therefore, the objective of this article is to address these limitations by conducting a comprehensive examination of fault-induced behavior changes in the Lorenz system. The article aims to shed light on the significance of fault detection and its implications.

This paper investigates the effects of process faults on each of the parameters of the chaotic Lorenz system. These faults have the potential to completely alter the dynamics of the system, leading to bifurcations, changes in fixed points, or even system instability. The objective of this article is to analyze and identify the behavioral changes in the system resulting from these specific faults. Additionally, it aims to emphasize the significance of timely detection and identification of faults to prevent failures and disasters in industrial systems. Furthermore, the paper examines the simultaneous impact of sensor and process faults and disturbances on the system behavior. The states and faults are estimated using the reduced-order observer proposed in [35]. To summarize, this paper's contributions can be condensed into two main aspects:

Analyses the influence of process faults on all parameters of the chaotic Lorenz system.

Highlights how these faults can significantly alter the system's dynamic behavior, leading to bifurcation, alterations in fixed points, or even system instability.

Notably, this research provides a more comprehensive analysis compared to existing papers, as it explores aspects that have not been extensively studied before.

The paper structure consists of the following sections. The homoclinic orbit in the Lorenz system is examined with the specified initial conditions and without input in section 2. TS fuzzy reduced-order observer is introduced in Section 3. In section 4, the effect of process faults on each of the system parameters is investigated and the faults are detected by the observer. And in the following, sensor and process faults, and disturbances affect simultaneously on the system, and they are estimated using the observer. Finally, in Section 5, the result of the article is described.

2- HOMOCLINIC ORBITS IN LORENZ SYSTEM

If a path $X(x : r^*)$ starts at a point x_0, which is not on the stable manifold, and reaches x_1 at a given time t_1. The same X path is expected to arrive at the x_1-neighborhood at the same time t_1, starting from the initial condition $x_0 \pm \epsilon$, which is perturbation small enough. Since the stable manifold comprises the z-axis, its perturbation causes the path to $C\pm$ to be sent, which depends on the direction of the perturbation. The unexpected result is that if the perturbation, though small, occurs in the parametric space, the path will converge to another fixed point. For example, $X(x; (r^*, b, \sigma)) \rightarrow C+$, while $X(x; (r^*+\delta, b, \sigma)) \rightarrow C-$.

The concept of a homoclinic orbit can be explained by the variation in direction resulting from a small change in the parameter space. Precise calculation of these orbits is difficult due to their susceptibility to round-off errors and constraints associated with machine precision. However, they can be numerically observed with minor perturbations. As a result, it is anticipated that a homoclinic bifurcation may occur in the Lorenz system, as discussed in the study by Hateley et al. [33]. This article examines the aforementioned concept within the context of the Lorenz system. The Lorenz system equation is as follows, which has three parameters b, r, and σ.

$$\begin{cases} \dot{x}_1(t) = \sigma\left(x_2 - x_1\right) \\ \dot{x}_2(t) = r x_1 - x_2 - x_1 x_3 \\ \dot{x}_3(t) = x_1 x_2 - b x_3 \end{cases} \tag{1}$$

The σ and b parameters are constant, ($\sigma = 10$, $b = 8/3$) [32]. At $r = r_{hom} \simeq 13.9162$, as shown in Figure 1, unstable saddle separators come back to the origin and, therefore, constitute a homoclinic butterfly. This creates a "homoclinic explosion" in the model phase space, which is filled at once with many countable periodic orbits that make most of the Lorenz attractor structure.

When the value of r is equal to $r_{AH} \simeq 24.7368$, is described in [20]. For more information on the rest of the r values (for example, $r_{het} \simeq 24.0579$), refer to [36] .

The behavior of the system is examined by varying the r parameter value, and two different initial conditions, $x_{01} = (1.e-16, 1.e-16, 1.e-16)$ and $x_{02} = (1.e-16, -1.e-16, 1.e-16)$, in two scenarios. It should be noted that the second array in the initial condition x_{02} is negative. The Lorenz dynamics (1) has two kinds of fixed points. One of the fixed points for all values of the parameters is the origin $(x_1^*, x_2^*, x_3^*) = (0, 0, 0)$. Other fixed points for $r > 1$ are a symmetric pair of fixed points $(x_1^* = x_2^* = \pm\sqrt{b\left(r-1\right)}, x_3^* = r-1)$. The first and second states converge to the same value. Therefore, in the following figures, only the first state is plotted.

Scenario 1: In this scenario, the behavior of the system is investigated for $r = 13.9265$. Phase plane and state trajectories of the system are shown in Figure 2 and 3. After a while,

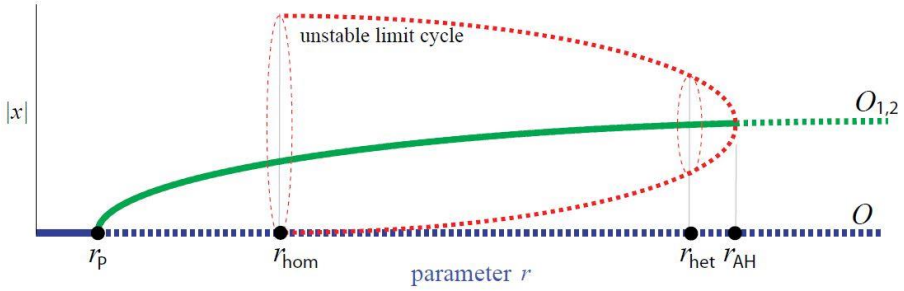

Fig. 1. The bifurcation diagram for the Lorenz equation [36]

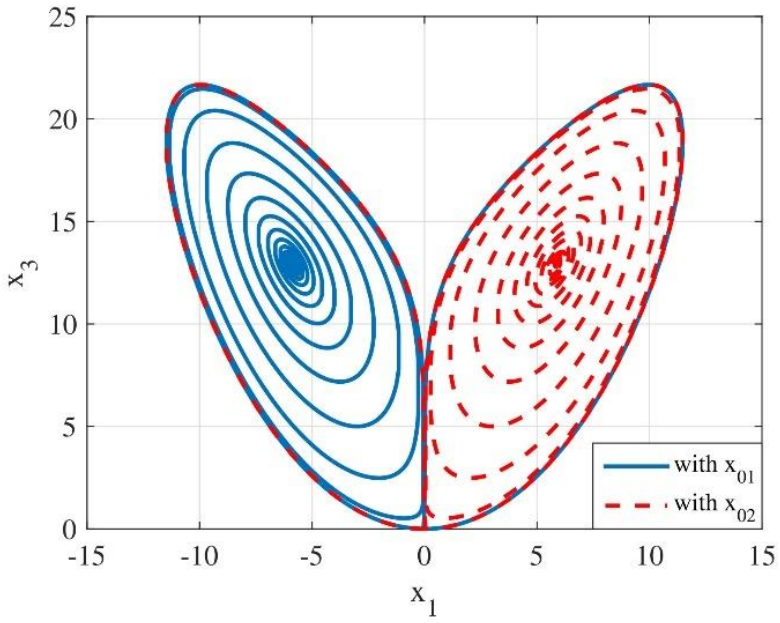

Fig. 2. Phase plane behavior of the state variables x1 and x3 when r = 13.9265 (Scenario 1)

the trajectories of states converge to the fixed points. The sensitivity to the initial conditions in the figure is well seen. The sign of the initial condition of the second state changes and thus states flow towards two different fixed points. They converge to the value $x_1^* = x_2^* = -\sqrt{b(r-1)} = -5.87$ with the initial conditions x_{01} and converge to the $x_1^* = x_2^* = +\sqrt{b(r-1)} = +5.87$ with the initial conditions x_{02}. With both initial conditions, the value of the third state converges to $x_3^* = r - 1 = 12.9265$.

Scenario 2: In this scenario, the system behavior is considered for $r = 13.91$, The Phase plane and state trajectories of the system are shown in Figures 4 and 5. After an initial transient, the state trajectories with x_{01} converge to the fixed point ($x_1 = x_2 = 5.8674$, $x3 = 12.91$) and with x_{02} converge to the fixed point ($x_1 = x_2 = -5.8674$, $x_3 = 12.91$). The r parameter has changed slightly, but the results are completely opposite to those obtained in the previous scenario.

In scenarios 1 and 2, the values of r were selected in such a way that in one scenario they are slightly lower than r_{hom}, and in the other scenario they are slightly higher than r_{hom}. This choice was made to accurately describe the behavior of hemoclinic orbits and hemoclinic explosions. According to what was examined in this section of the paper, the sensitivity of the Lorenz system to the initial conditions was shown, where small variations led to huge results in the future, which is raised in the chaos theory that studies the behavior of dynamic systems [37]. In this section, we examined the effect of changing the r parameter and the initial conditions on the system. In the following, we will examine the effect of various process faults on the system and its diagnosis.

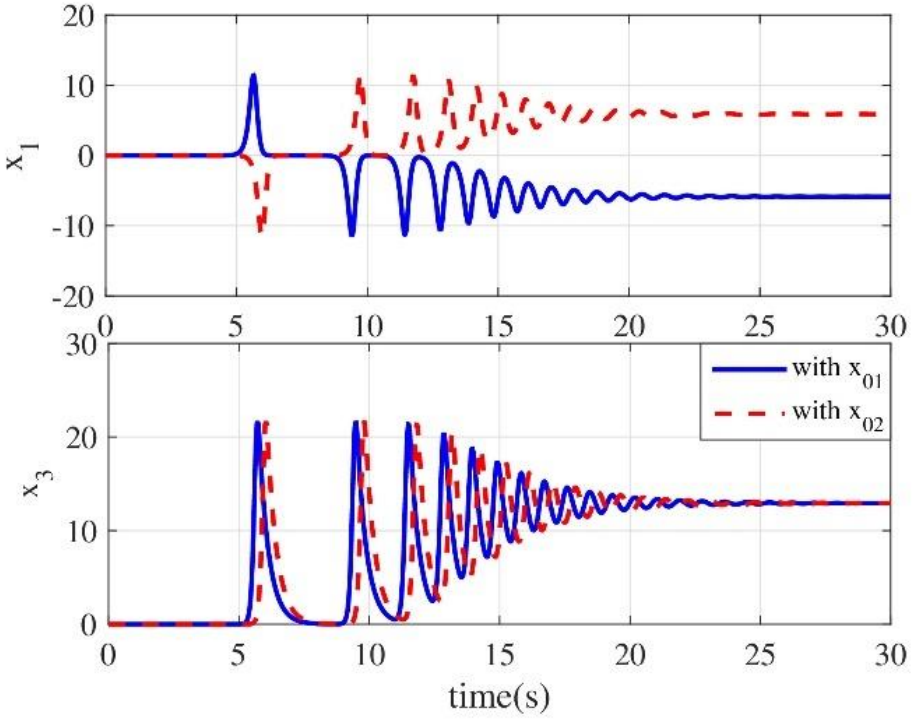

Fig. 3. The trajectory of states when r = 13.9265 (Scenario 1)

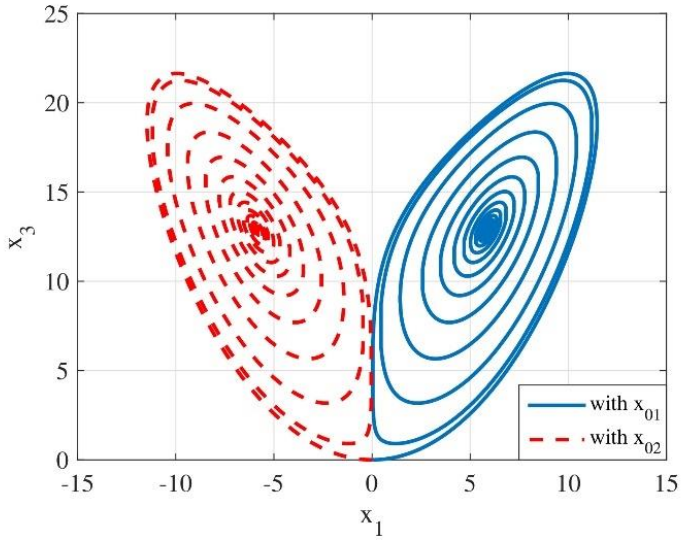

Fig. 4. Phase plane behavior of the state variables x1 and x3 when r = 13.91 (Scenario 2)

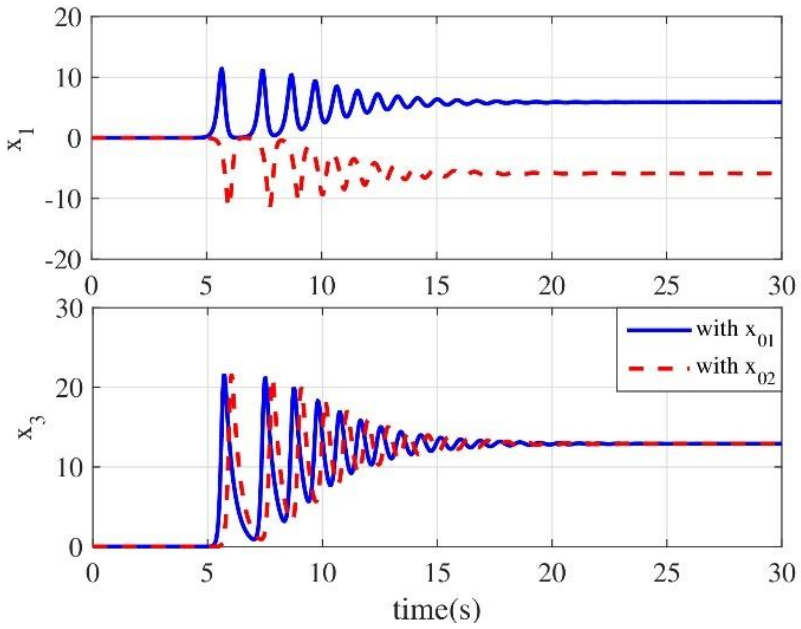

Fig. 5. The trajectory of states with r = 13.91 (Scenario 2)

3- FAULT DETECTION

In this section, the goal is to diagnose process faults in the system, so first an observer that can estimate the states and faults is introduced. Then the effect of process faults on each of the system parameters is investigated and the faults that have occurred are detected by using the introduced observer.

3- 1- REDUCED ORDER OBSERVER

A TS Fuzzy model of a noisy nonlinear system with process and sensor faults is expressed by:

$$\begin{cases} \dot{x}(t) = \sum_{i=1}^{r_F} \xi_i \left(A_i x(t) + B_i u(t) + F_i f_p(t) + H_i w(t) \right) \\ y(t) = \sum_{i=1}^{r_F} \xi_i \left(C_i x(t) + F_{si} f_s(t) \right) \end{cases} \quad (2)$$

x(t), u(t), f (t) are the system state vector, known input vector, and the faults, respectively. *ζi* stands for *ζi(x)* representing system membership functions.

A new variable x_m is considered and the fuzzy model (2) is rewritten according to [35],

$$\begin{cases} M\dot{x}_m(t) = \sum_{i=1}^{r_F} \xi_i \left(A_{mi} x_m(t) + B_{mi} u(t) + F_{mi} f_p(t) + H_{mi} w(t) + F_m f_s(t) \right) \\ y(t) = \sum_{i=1}^{r_F} \xi_i C_m x_m(t) \end{cases} \quad (3)$$

where

$$x_m(t) = \begin{bmatrix} x(t) \\ f_s(t) \end{bmatrix}, \; M = \begin{bmatrix} I_n & 0 \\ 0 & 0 \end{bmatrix},$$

$$A_{mi} = \begin{bmatrix} A_i & 0 \\ 0 & -F \end{bmatrix}, \; F_{mi} = \begin{bmatrix} F_i \\ 0 \end{bmatrix},$$

$$B_{mi} = \begin{bmatrix} B_i \\ 0 \end{bmatrix}, \quad H_{mi} = \begin{bmatrix} H_i \\ 0 \end{bmatrix},$$

$$F_{msi} = \begin{bmatrix} 0 \\ F_{si} \end{bmatrix}, \quad C_{mi} = \begin{bmatrix} C & F \end{bmatrix}$$

Add $L_{mi}\dot{y}$ to both sides of the Eq. (3),

$$\begin{cases} \dot{x}_m(t) = \sum_{i=1}^{r_F} \xi_i \left(\tilde{A}_{mi} x_m(t) + \tilde{B}_{mi} u(t) + \tilde{F}_{mi} f_p(t) + \tilde{H}_{mi} w(t) + \tilde{F}_{msi} f_s(t) + M^{-*}_{mi} L_{mi} \dot{y}(t) \right) \\ y(t) = \sum_{i=1}^{r_F} \xi_i \tilde{C}_{mi} x_m(t) \end{cases} \quad (4)$$

where

$$\tilde{A}_{mi} = \bar{M}_{mi}^{*} A_{mi}, \quad \tilde{B}_{mi} = \bar{M}_{mi}^{*} B_{mi},$$
$$\tilde{F}_{mi} = \bar{M}_{mi}^{*} F_{mi}, \quad \tilde{H}_{mi} = \bar{M}_{mi}^{*} H_{mi},$$
$$\tilde{F}_{msi} = \bar{M}_{mi}^{*} F_{msi}$$

$$\bar{M}_{mi}^{*} = \begin{bmatrix} I & 0 \\ -F^{-}C & F^{-}\tilde{L}_i^{-1} \end{bmatrix},$$
$$\tilde{L}_i^{-1} = diag\left(\lambda_{i1}, ..., \lambda_{iq}\right),$$
$$\bar{M}_{mi}^{*} L_{mi} = \begin{bmatrix} 0 \\ F^{-} \end{bmatrix}$$

It is stated in [35] that under some conditions the transformation matrix, R, can be expressed as follows.

$$R = \begin{bmatrix} C_m^{\perp T} \\ C_m \end{bmatrix}^{-1}, \quad x_m(t) = Rr(t)$$

Using the new variable $r(t)$, which is obtained by the transformation matrix, Eq. (4) can be rewritten as

$$\begin{cases} \dot{r}(t) = \sum_{i=1}^{r_F} \xi_i \left(\bar{A}_i r(t) + \bar{B}_i u(t) + \bar{F}_i f_p(t) + \right. \\ \qquad \left. \bar{H}_i w(t) + \bar{F}_{si} f_s(t) + Q\dot{y}(t)\right) \\ y(t) = \sum_{i=1}^{r_F} \xi_i \bar{C}_m R r(t) = \begin{bmatrix} 0 & I \end{bmatrix} r(t) \end{cases} \tag{5}$$

Where

$$\bar{A}_i = R^{-1}\tilde{A}_{mi}R, \quad \bar{B}_i = R^{-1}\tilde{B}_{mi},$$
$$\bar{F}_i = R^{-1}\tilde{F}_{mi}, \quad \bar{H}_i = R^{-1}\tilde{H}_{mi}$$

$$Q = R^{-1}\bar{M}_{mi}^{*} L_{mi}, \quad \bar{F}_{si} = R^{-1}\tilde{F}_{msi},$$
$$Q = R^{-1}\begin{bmatrix} 0 \\ F^{-} \end{bmatrix}$$

Eq. (5), given that the variable r is independent of or dependent on the measured output, is decomposed as follows.

$$\begin{cases} \dot{r}_1(t) = \sum_{i=1}^{r_F} \xi_i \left(A_{11i} r_1(t) + A_{12i} r_2(t) + \right. \\ \bar{B}_{1i} u(t) + \bar{F}_{1i} f_p(t) + \bar{H}_{1i} w(t) + \\ \left. \bar{F}_{1si} f_s(t) + Q_1 \dot{y}(t)\right) \\ \dot{r}_2(t) = \sum_{i=1}^{r_F} \xi_i \left(A_{21i} r_1(t) + A_{22i} r_2(t) + \right. \\ \bar{B}_{2i} u(t) + \bar{F}_{2i} f_p(t) + \bar{H}_{2i} w(t) + \\ \left. \bar{F}_{2si} f_s(t) + Q_2 \dot{y}(t)\right) \\ y(t) = \begin{bmatrix} 0 & I \end{bmatrix} \begin{bmatrix} r_1(t) \\ r_2(t) \end{bmatrix} = r_2(t) \end{cases} \tag{6}$$

Where

$$r(t) = \begin{bmatrix} r_1(t) \\ r_2(t) \end{bmatrix}, \quad \begin{bmatrix} A_{11i} & A_{12i} \\ A_{21i} & A_{22i} \end{bmatrix} = \bar{A}_i,$$
$$\begin{bmatrix} \bar{B}_{1i} \\ \bar{B}_{2i} \end{bmatrix} = \bar{B}_i, \quad \begin{bmatrix} \bar{F}_{1i} \\ \bar{F}_{2i} \end{bmatrix} = \bar{F}_i,$$
$$\begin{bmatrix} \bar{H}_{1i} \\ \bar{H}_{2i} \end{bmatrix} = \bar{H}_i, \quad \begin{bmatrix} \bar{F}_{1si} \\ \bar{F}_{2si} \end{bmatrix} = \bar{F}_{si}$$

Given the above equations, the sensor fault $f_s(t)$ is expressed as follows.

$$x_m(t) = \begin{bmatrix} x(t) \\ f_s(t) \end{bmatrix} =$$
$$Rr(t) = \begin{bmatrix} R_{11} & R_{12} \\ R_{21} & R_{22} \end{bmatrix} \begin{bmatrix} r_1(t) \\ r_2(t) \end{bmatrix} \Rightarrow$$

$$f_s(t) = R_{21} r_1(t) + R_{22} r_2(t)$$

A reduced-order fuzzy estimator is proposed in [35] for r_1 and f_p as follows,

$$
\begin{cases}
\hat{r}_1(t) = z_1(t) + \sum_k \left[\left(Q_1 + K_{2k} - K_{2k} Q_2 \right) y(t) \right] \\
\hat{f}_a(t) = z_2(t) + \sum_k \left[\left(K_{3k} - K_{3k} Q_2 \right) y(t) \right] \\
\dot{q}_1(t) = \sum_{i,j,k}^{r_F} [(A_{11i} - K_{2j} A_{21i}) q_1(t) + \\
(\bar{B}_{1i} - K_{2j} \bar{B}_{2i}) u(t) + (\bar{F}_{1i} - K_{2j} \bar{F}_{2i}) \hat{f}_a(t) + \\
((A_{11i} - K_{2j} A_{21i})(Q_1 + K_{2k} - K_{2k} Q_2) + \\
(A_{12i} - K_{2j} A_{22i})) y(t)] \\
\dot{q}_2(t) = \sum_{i,j,k}^{r_F} [-K_{3j} F_{2i} q_2(t) \\
-K_{3j} A_{21i} \hat{r}_1(t) - K_{3j} \bar{B}_{2i} u(t) \\
+(-K_{3j} F_{2j} (K_{3k} - K_{3k} Q_2) - \\
K_{3j} A_{22i}) y(t)]
\end{cases}
\tag{7}
$$

The fuzzy estimator error dynamics are asymptotically stable with H_∞ performance level μ, if there is a positive matrix P and satisfy the following linear matrix inequality.

$$
G_{ii} < 0, \quad \frac{2}{r_F - 1} G_{ii} + G_{ij} + G_{ji} < 0, \quad 1 \le i \ne j \le r_F \tag{8}
$$

Where $e(t) = [(r_1(t) - \hat{r}_1(t))^T, \quad (f_p(t) - \hat{f}_p(t))^T]^T$

$$
G_{ij} = \begin{bmatrix} \bar{A}_i^T P + P \bar{A}_i - J_j^T Q_i^T - Q_i J_i + T_1 & P\bar{H}_i - Q_i J_i \\ * & -\mu T_2 \end{bmatrix}
$$

$$
\int_0^t e^T(s) T_1 e(s) ds < \mu \int_0^t \delta^T(s) T_2 \delta(s) ds, \quad if \quad \delta(t) \ne 0
$$

Then the estimator gain matrix is obtained as follows

$$
K_i = P^{-1} Q_i \tag{9}
$$

For more details on this observer, refer to this paper [35].

4- Simulations

This section is divided into two parts. The first part aims to explore how process faults impact each of the system parameters in the Lorenz system. It involves analyzing the sensitivities of the parameters and showcasing the various effects of faults on the system, leading to noticeable changes in behavior. The states and faults are estimated using the observer discussed in the previous section. In the second part, we investigate the combined impact of disturbances, process faults, and sensor faults.

4- 1- Process Fault

A process fault $f_p(t)$ directly affects the parameters of the physical system and makes the dynamic behavior inappropriate. In the Lorenz system, process fault can occur in each of the parameters r, b, and σ.

$$
\begin{cases}
\dot{x}_1(t) = (\sigma + f_\sigma)(x_2 - x_1) \\
\dot{x}_2(t) = (r^* + f_r) x_1 - x_2 - x_1 x_3 \\
\dot{x}_3(t) = x_1 x_2 - (b + f_b) x_3
\end{cases}
\tag{10}
$$

In this section, the behavior of the system is investigated for the effect of the process fault on each of the parameters r, b, and σ. States of the system are estimated by the observer briefly explained in the previous section. The fuzzy model of the Lorenz system can be achieved from [38].

The initial state is set to be x_{01} and the initial estimator values are assigned at $x = [0; 0; 0]$. The

value of the parameters is $(r^* = 13.91, \sigma = 10, b = 8/3)$. The behavior of the system with these numerical values and the initial condition x_{01} is explained in scenario 2 of the second section, so it is expected that after an initial transient, the state trajectories converge to this fixed point $(x_1 = x_2 = 5.8674, x_3 = 12.91)$.

In the following, three consequences of process faults on the system are examined.

A. homoclinic explosion

In this part, we explore the impact of a process fault on the parameter *r* in the system. A process fault with $f_r = 0.5$ occurs at $t = 5$ seconds. Figure 6 shows the state trajectories of the system and their corresponding estimates. As can be seen from the figure, the states of the system are well estimated by the observer. Therefore, according to the state's path, the change in system behavior at $t = 5$ sec is visible, and contrary to what was expected, the states converged to another fixed point $(x_1 = x_2 = -5.8674, x_3 = 12.91)$. This change in system behavior indicates the occurrence of a homoclinic bifurcation in the system. Initially, the value of $r^* = 13.91$, but due to the fault, the system behavior demonstrates a higher value for the *r* parameter. To provide a clearer representation of the homoclinic explosion, the system's phase plane is depicted in Figure 7.

B. Chaotic behavior

In this part, the effect of process fault $f_r = 3$ at $t = 12$ sec on the parameter *r* is investigated. Prior to the occurrence of the fault, the states of the system were rotating around a fixed point and would have converged. However, with the process fault occurring at $t = 12$ seconds, the system exhibited chaotic behavior.

Figure 8 shows the state trajectories of the system and their estimate. The accuracy of the estimation is evident even in the presence of chaotic behavior and intense fluctuations

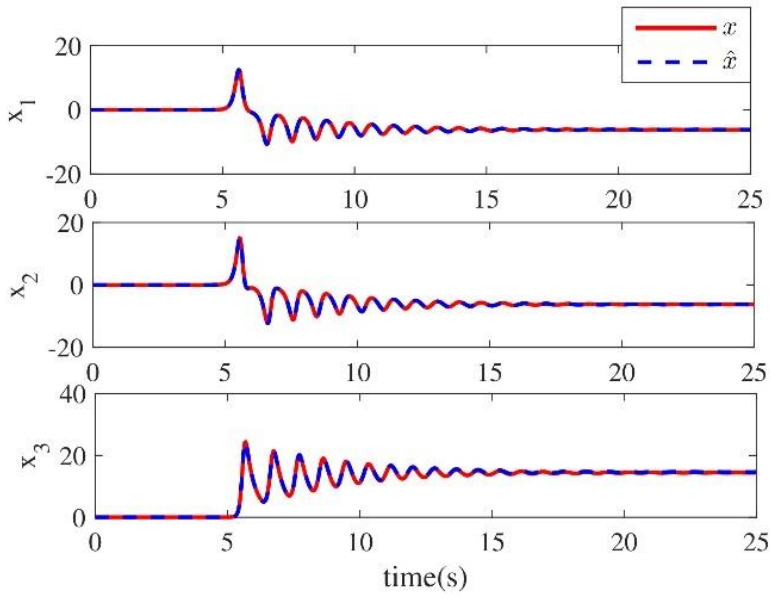

Fig. 6. The trajectory of states when r = 13.91 with fr = 0.5 at t = 5 sec

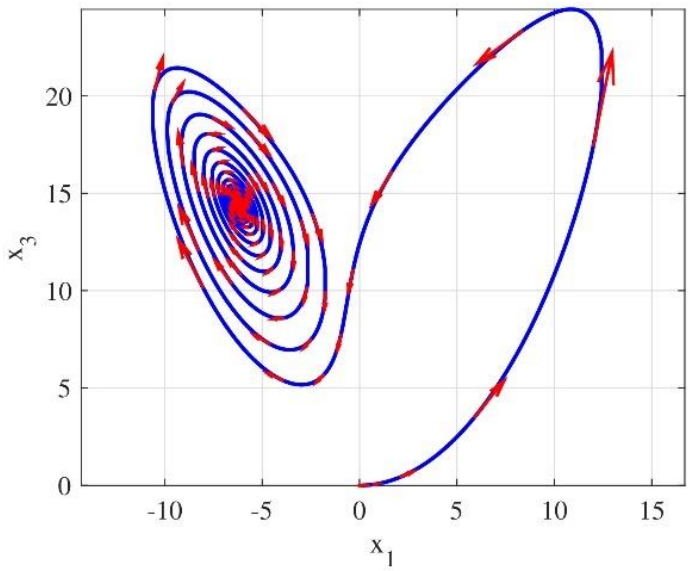

Fig. 7. Phase plane behavior of the state variables x1 and x3 when r = 13.91 with fr = 0.5 at t = 5 sec.

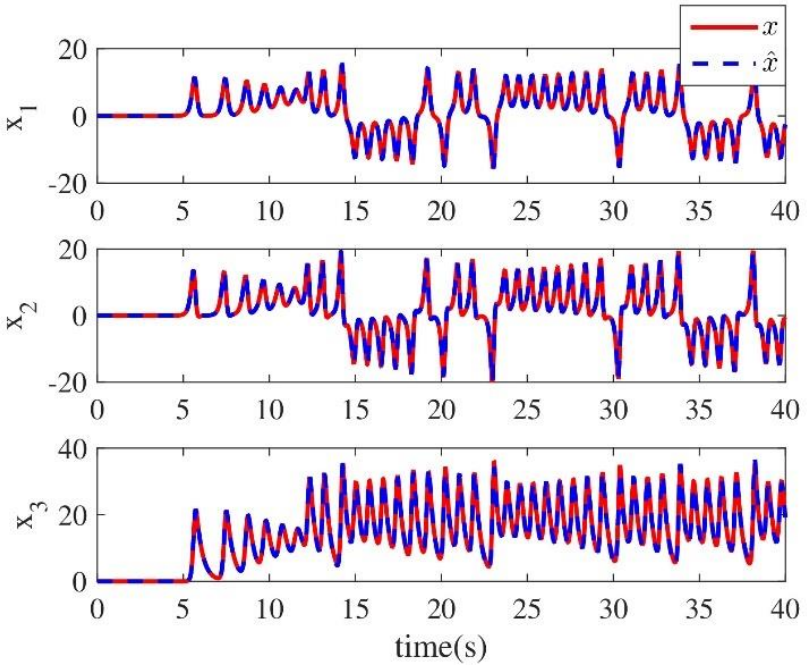

Fig. 8. The trajectory of states when r = 13.91 with fr = 3 at t = 12 sec

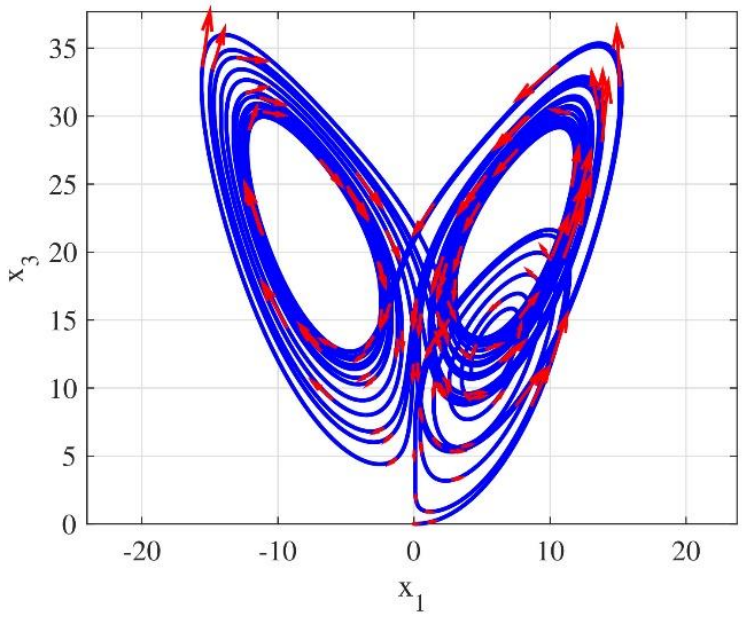

Fig. 9. Phase plane behavior of the state variables x1 and x3 when r = 13.91 with fr = 3 at t = 12 sec.

in the system states, as depicted in the figure. The phase plane of the system is shown in Figure 9. The process fault and the estimation are displayed in Figure 10. As Eq. (10) indicates, the process fault signal is derived from $f_p(t) = f_r x_1(t)$.

C. Unstable behavior

In this part, we investigate the impact of a process fault, denoted as $f_b = 3$, occurring at $t = 12$ seconds, on the parameter b in the system. The phase plane of the system is depicted in Figure 11. The figure illustrates that the states of the system

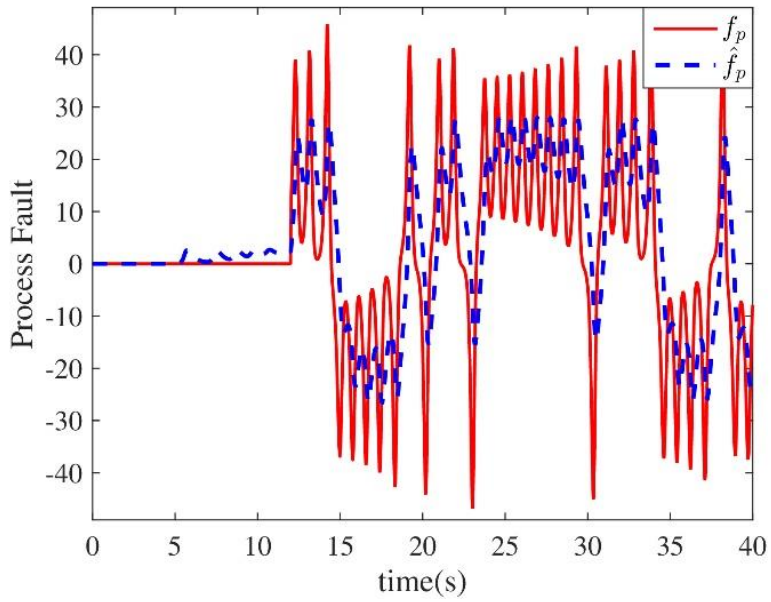

Fig. 10. Process fault and the estimation

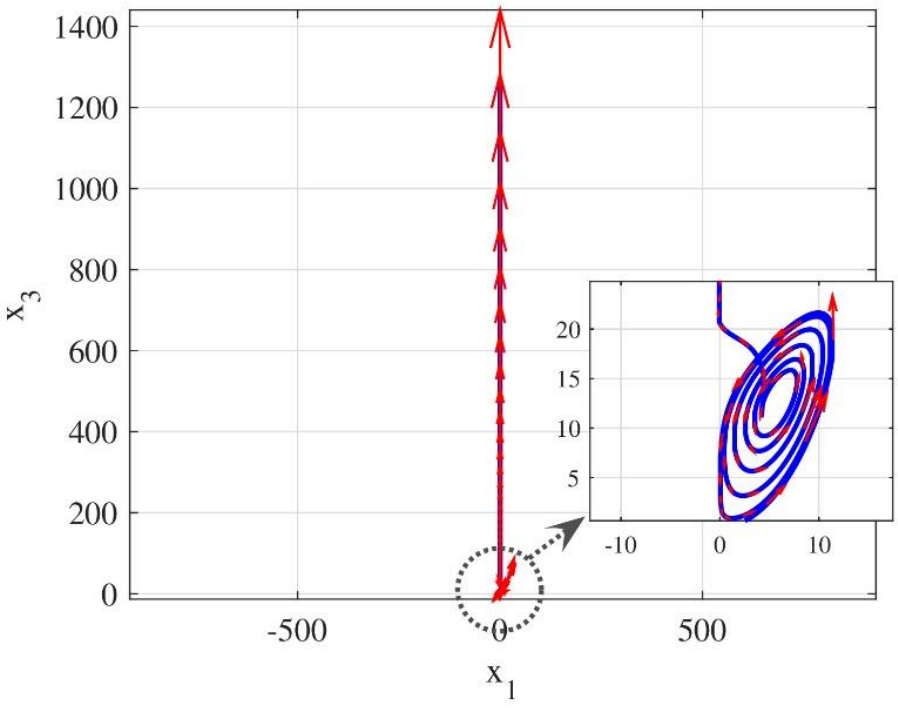

Fig. 11. Phase plane behavior of the state variables x1 and x3 when r = 13.91 with fb = 3 at t = 12 sec

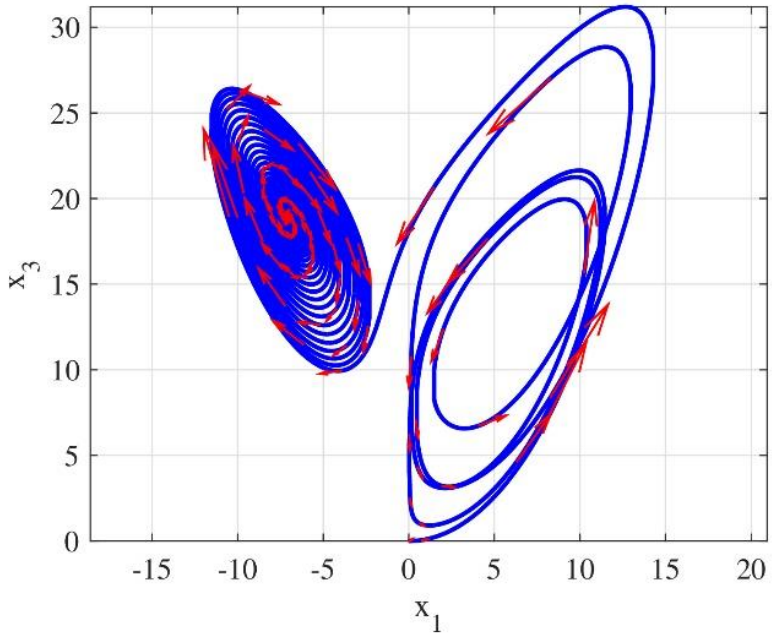

Fig. 12. Phase plane behavior of the state variables with disturbance and fr = 2 at t = 5 sec

initially rotate around a fixed point and converge. However, the occurrence of the process fault at $t = 12$ seconds leads to system instability, causing the state x_3 to immediately diverge towards infinity.

It should be noted that if the process fault affects the parameter $f_\sigma = 0.5$, it does not significantly impact the system behavior. This is because the states x_1 and x_2 are equal, and according to the Lorenz system Eq. (10), the parameter σ influences the difference between these two states.

4- 2- Process fault with disturbance and sensor fault

In this section of the paper, we investigate the impact of a process fault on the system's behavior in the presence of simultaneous disturbance and sensor fault. Specifically, we assume that at time $t = 5$ seconds, the process fault $f_r = 2$ affects the parameter r. Additionally, a sine signal with an amplitude of 2 and a frequency of 3000 is considered as a disturbance in the system $(w(t) = 2 \sin(3000t))$. Figures 12 and 13 show the phase plane and the state trajectories of the system, along with their estimates. As can be seen in the figures, at the moment of fault occurrence, the rotation path of the homoclinic orbit changes, and the states flow towards another fixed point. Figure 14 displays the sensor fault signal and the estimation, which includes ramp, step, and sinusoidal signals. However, upon observing the system's states, it is evident that there is no substantial change in the system's behavior following the sensor fault. This highlights the significance of thoroughly examining process faults to ensure system reliability. Also, by estimating the states of the system, the behavior of the system is revealed, so that the fault propagating in the system and causing failure can be prevented.

5- Conclusion

This paper begins by elucidating the homoclinic orbits within the Lorenz system and underscores the system's sensitivity to initial conditions. Subsequently, an examination of process faults is conducted, where small variations in each parameter induce homoclinic bifurcations, changes in fixed points, or system instability. Knowing the dynamic behavior of the system shows that these problems are not far from the mind. This paper addresses these problems by estimating states and identifying faults using a fuzzy reduced-order observer. As a result, failure and catastrophe in the system can be prevented by enabling timely identification of faults. At the end of the article, sensor and process faults, and disturbances affect simultaneously on the system, and they are estimated using the observer. Nevertheless, upon scrutiny of the system's states, it becomes apparent that there is no significant alteration in the system's behavior subsequent to the occurrence of the sensor fault. This emphasizes the importance of a comprehensive investigation into process faults to guarantee the reliability of the system.

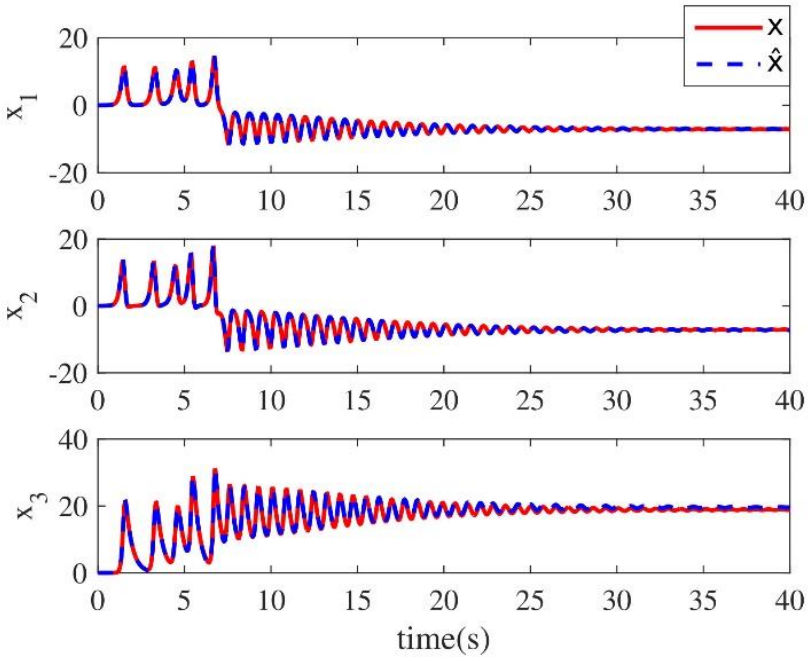

Fig. 13. The trajectory of states with disturbance and fr = 2 at t = 5 sec

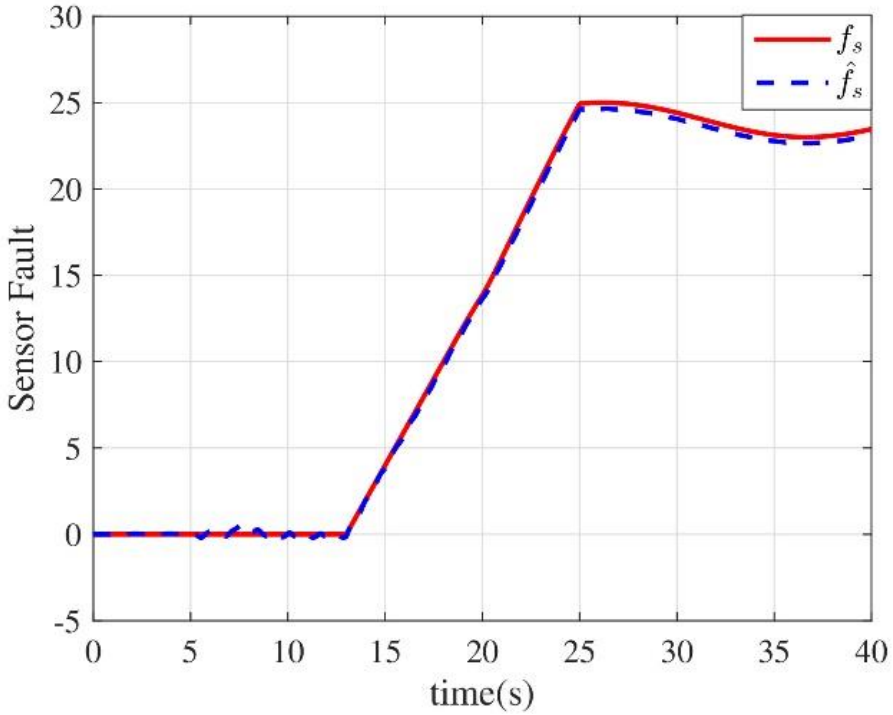

Fig. 14. Sensor fault and the estimation

References

[1] Liu, C., et al., Hierarchical-structure-based fault estimation and fault-tolerant control for multiagent systems. IEEE Transactions on Control of Network Systems, 2018. 6(2): p. 586--597.

[2] Kordestani, M., et al., Failure prognosis and applications—A survey of recent literature. IEEE transactions on reliability, 2019. 70(2): p. 728-748.

[3] Ding, S.X., Model-based fault diagnosis techniques: design schemes, algorithms, and tools. 2008.

[4] Doraiswami, R., C.P. Diduch, and J. Tang, A new diagnostic model for identifying parametric faults. IEEE transactions on control systems technology, 2009. 18(3): p. 533--544.

[5] Ma, L., et al., Fault tolerant control for a class of nonlinear system with actuator faults. Asian Journal of Control, 2021. 23(1): p. 474--485.

[6] Zhu, J.-W., et al., Fault estimation for a class of nonlinear systems based on intermediate estimator. IEEE Transactions on Automatic Control, 2015. 61(9): p. 2518--2524.

[7] Boem, F., et al., Distributed fault detection for interconnected large-scale systems: A scalable plug \& play approach. IEEE Transactions on Control of Network Systems, 2018. 6(2): p. 800--811.

[8] Han, J., et al., Fault estimation and fault-tolerant control for switched fuzzy stochastic systems. IEEE Transactions on Fuzzy Systems, 2018. 26(5): p. 2993--3003.

[9] Zhang, L., et al., Observer-based adaptive decentralized fault-tolerant control of nonlinear large-scale systems with sensor and actuator faults Nonlinear robust fault reconstruction and estimation using a sliding mode observer. IEEE Transactions on Industrial Electronics, 2018. 66(10): p. 8019--8029.

[10] Mu, Y., et al., Integrated design of robust fault estimation and fault-tolerant control against simultaneous actuator and sensor faults. Asian Journal of Control, 2021. 23(1): p. 341--350.

[11] Patton, R.J., P.M. Frank, and R.N. Clark, Issues of fault diagnosis for dynamic systems. 2013.

[12] Yan, X.-G. and C. Edwards, Nonlinear robust fault reconstruction and estimation using a sliding mode observer. Automatica, 2007. 43(9): p. 1605-1614.

[13] Zhang, X., M.M. Polycarpou, and T. Parisini, Fault diagnosis of a class of nonlinear uncertain systems with Lipschitz nonlinearities using adaptive estimation. Automatica, 2010. 46(2): p. 290--299.

[14] Li, L., et al., Diagnostic observer design for TS fuzzy systems: Application to real-time-weighted fault-detection approach. IEEE Transactions on Fuzzy Systems, 2017. 26(2): p. 805--816.

[15] Mehdi, R. and S. Zahra, Robust L1 observer design and circuit implementation for a class of faulty nonlinear systems. International Journal of Systems Science, 2023. 54(1): p. 113-123.

[16] 16. Fault detection and isolation of gas turbine engine using inversion-based and optimal state observers. European Journal of Control, 2020. 56: p. 206-217.

[17] Youssef, T., et al., Actuator and sensor faults estimation based on proportional integral observer for TS fuzzy model. Journal of the Franklin Institute, 2017. 354(6): p. 2524--2542.

[18] Garca, C.M., et al., Robust fault estimation based on interval Takagi-Sugeno unknown input observer. IFAC-PapersOnLine, 2018. 51(24): p. 508--514.

[19] Alia, R.S., C.S. Susan, and E.Y. Edwin, State Estimation in the Presence of Intermittent Actuator Faults. IFAC-PapersOnLine, 2020. 53(2): p. 2403-2408.

[20] Shams, Z. and A. Shahmansoorian, Fault estimation based on observer for chaotic Lorenz system with bifurcation problem. Transactions of the Institute of Measurement and Control, 2020. 42(3): p. 576--585.

[21] Lorenz, E.N., Deterministic nonperiodic flow. Journal of atmospheric sciences, 1963. 20(2): p. 130--141.

[22] Chen, G. and T. Ueta, Yet another chaotic attractor. Internat J Bifur Chaos, 1999. 9: p. 1465-6.

[23] Bridge the gap between the Lorenz system and the Chen system. International Journal of Bifurcation and Chaos, 2002. 12(12): p. 2917--2926.

[24] Pecora, L.M. and T.L. Carroll, Synchronization of chaotic systems. Chaos: An Interdisciplinary Journal of Nonlinear Science, 2015. 25(9): p. 097611.

[25] Nayfeh, A.H. and B. Balachandran, Applied nonlinear dynamics: analytical, computational, and experimental methods. 2008.

[26] Hilborn, R.C. and et al., Chaos and nonlinear dynamics: an introduction for scientists and engineers. 2000.

[27] Li, C., J.C. Sprott, and W. Thio, Linearization of the Lorenz system. Physics Letters A, 2015. 379(10-11): p. 888--893.

[28] Gao, R., A novel track control for Lorenz system with single state feedback. Chaos, Solitons \& Fractals, 2019. 122: p. 236--244.

[29] Luo, R., H. Su, and Y. Zeng, Chaos control and synchronization via switched output control strategy. Complexity, 2017. 2017.

[30] Mekircha, N., A. Boukabou, and N. Mansouri, Fuzzy control of original UPOs of unknown discrete chaotic systems. Applied Mathematical Modelling, 2012. 36(10): p. 5135--5142.

[31] Mohammadpour, S. and T. Binazadeh, Robust finite-time synchronization of uncertain chaotic systems: application on Duffing-Holmes system and chaos gyros. Systems Science \& Control Engineering, 2018. 6(1): p. 28--36.

[32] Strogatz, S.H., Nonlinear dynamics and chaos: with applications to physics, biology, chemistry, and

engineering. 2018.

[33] Hateley, J., The lorenz system. Lecture Notes,http: // web.math.ucsb.edu/jhate-ley/paper/lorenz.pdf 2019.

[34] Doedel, E.J., B. Krauskopf, and H.M. Osinga, Global invariant manifolds in the transition to preturbulence in the Lorenz system. Indagationes Mathematicae, 2011. 22(3-4): p. 222--240.

[35] Han, J., et al., Robust state/fault estimation and fault tolerant control for TS fuzzy systems with sensor and actuator faults. Journal of the Franklin Institute, 2016. 353(2): p. 615--641.

[36] Barrio, R., A. Shilnikov, and L. Shilnikov, Kneadings, symbolic dynamics and painting Lorenz chaos. International Journal of Bifurcation and Chaos, 2012. 22(04): p. 1230016.

[37] Boeing, G., Visual analysis of nonlinear dynamical systems: chaos, fractals, self-similarity and the limits of prediction. Systems, 2016. 4(4): p. 37.

[38] Chen, W. and M. Saif, Fuzzy nonlinear unknown input observer design with fault diagnosis applications. Journal of Vibration and Control, 2010. 16(3): p. 377-401.

HOW TO CITE THIS ARTICLE
Z. Shams, H. Zarabadipour, Process Fault and Homoclinic explosion in the Lorenz system, AUT J. Model. Simul., 55(2) (2023) 201-214.

DOI: 10.22060/miscj.2024.21827.5304